Stress derivation from earthquake focal mechanisms

A. Barth, J. Reinecker and O. Heidbach

1. Introduction

One of the most evident effects of stress release in the crust are tectonic earthquakes. Due to the large amount of existing earthquake focal mechanisms from regional studies and the steadily increasing number of CMT solutions made routinely public by e.g. the Global CMT Project (formerly by the Harvard seismology group) or the NEIC/USGS, single earthquake focal mechanisms (FMS) make up the majority of data records in the WSM database. Focal mechanism data provide information on the relative magnitudes of the principal stresses, so that a tectonic regime can be assigned.

The determination of principal stress orientations and relative magnitudes from these mechanisms must be done with appreciable caution. Three types of data records from focal mechanisms are distinguished in the WSM database: Single (FMS), formal inversions (FMF), and average/composite (FMA) focal mechanisms. The main difference between these in terms of stress indication is their reliability to indicate regional tectonic stress.

2. Single focal mechanisms (FMS)

2.1. Determination of FMS

Several methods for determining FMS are in use such as first motion of P waves, polarizations and amplitudes of S waves (e.g. Khattri, 1973), the analysis of P/S amplitude ratios (e.g. Kisslinger et al., 1981) and moment tensor inversion (e.g., Stein and Wysession, 2003). All these methods are using the radiation pattern of seismic rays that expresses the orientation of the active fault and the slip direction (Fig. 1). These patterns can be used to describe the kinematic processes in the seismic source. Here we focus on the most frequently used methods:

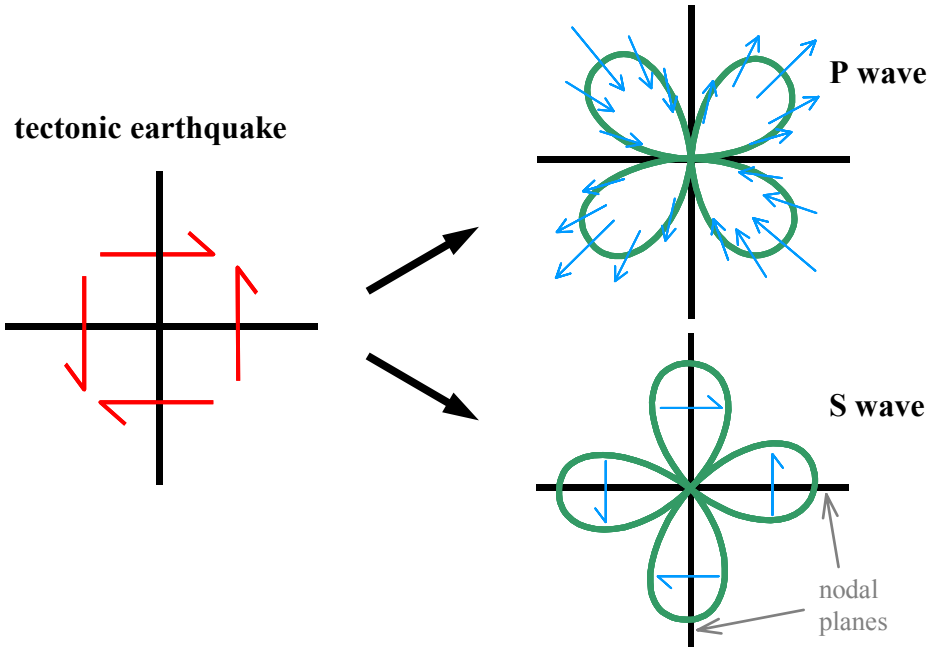

Figure 1: P and S wave radiation patterns of a double couple source.

2.1.1. First-motion of P waves

P-waves radiate relative to the focus with compressional or dilatational initial motion (Fig. 1). The signal changes in direction of the fault plane and the orthogonal auxiliary plane (both are called nodal planes). Along these planes there is no radiation of P-waves. The first onset of the P-wave on a seismogram of the vertical seismometer component is used to distinguish between a compressional and dilatational first motion of the wavefront. The observed first motion is then projected backwards along the ray path onto a conceptual homogeneous unit sphere around the focus (focal sphere), which is thought to be a point source at the very beginning of the rupture event. Any P-wave ray path leaving the source can be identified by two parameters: the azimuth from the source, ϕ, and the angle of emergence, i_0 (Fig. 2). The angle of emergence is a function of the distance, Δ, between the source and the recording station, and for near stations the crustal model in use. The geographic position of the seismometer is transferred on the focal sphere to a point where the tangent to the ray at the source intersects the focal sphere.

When all available data are plotted in the lower hemisphere of a stereographic projection, two orthogonal nodal planes separating compressional from dilatational first motion can be drawn. The axes of maximum shortening and maximum lengthening bisecting the quadrants are known as the P and the T axes, respectively. Thus, the axis are principal strain axes that must not necessarily coincide with the principal stress axes.

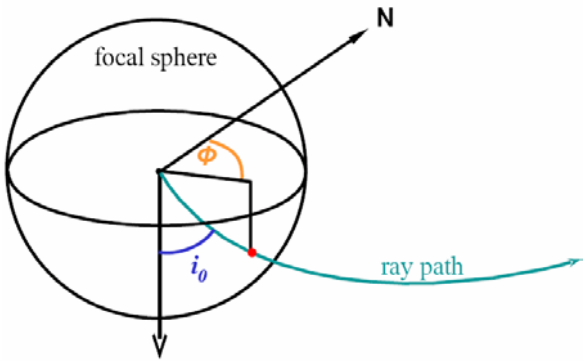

Figure 2: Focal sphere of an earthquake source. Shown is a ray path with azimuth ϕ and angle of emergence i_0.

The P axis lies within the quadrant of dilatational initial motions, whereas the T axis lies within the quadrant of compressional initial motions (Fig. 3). Both are perpendicular to the intersection of the two nodal planes. The axis formed by this intersection is called the B- or the null axis. The FMS is fully described by the orientation (dip direction and dip) of the P-, T-, and B-axes.

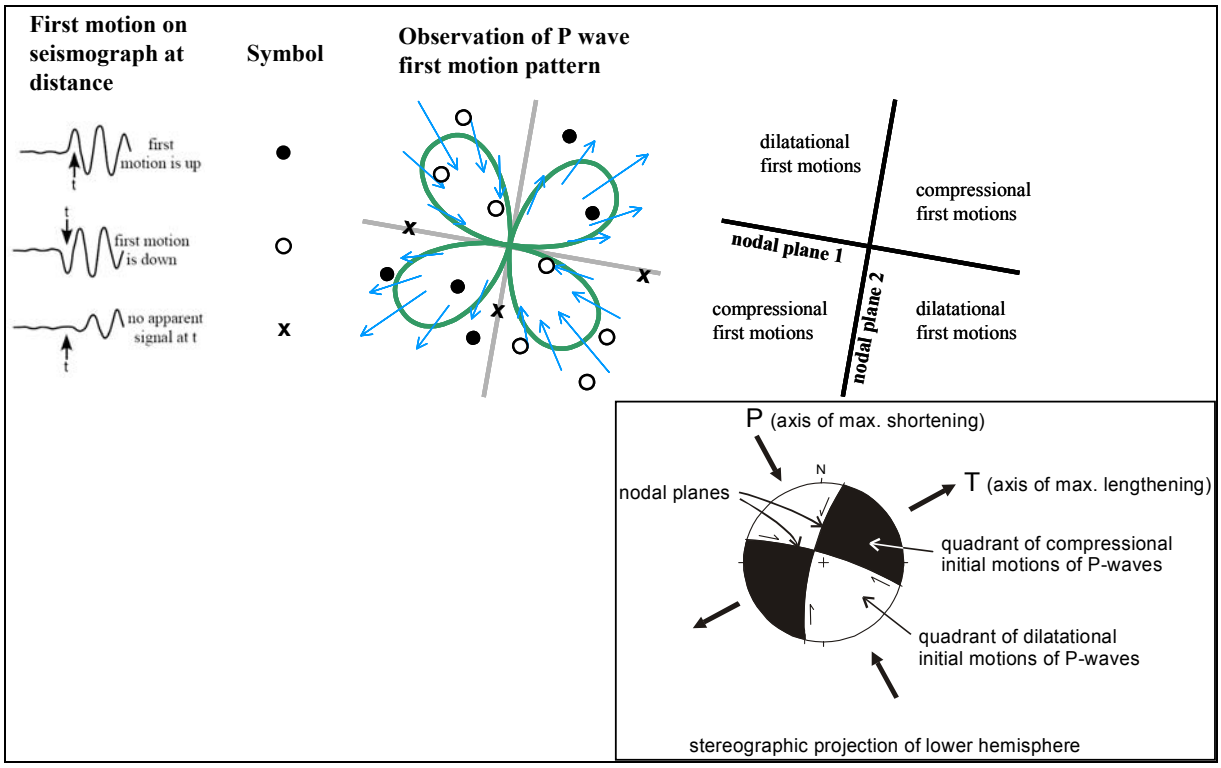

Figure 3: Elements of a fault plane solution (see text for more explanation).

2.1.2. Moment tensor inversion

Moment tensor inversion as well uses the radiation pattern of body- and/or surface-waves. However, here the complete waveform data is inverted to fit synthetic waveforms calculated for a reference earth model (e.g. Jost and Hermann, 1989). The seismic moment tensor ***M*** is a symmetric second order tensor, that describes a variety of seismic sources and consists of the nine couples of equivalent body forces (Fig. 4).

The off-diagonal elements are assigned to opposite forces that are offset in direction normal to their orientation and thus apply a net torque. However, because of the symmetry of the moment tensor, the conservation of angular momentum is guaranteed. The diagonal elements correspond to force dipoles

acting along the coordinate axes. If the earth's structure is known and waveform data is available, the seismic moment tensor ***M*** and thus the focal mechanism of an earthquake can be calculated by inversion. More detailed introductions on moment tensors can be found in Jost and Hermann (1989) or Stein and Wysession (2003) and various textbooks on seismology. Centroid moment tensors (CMT) include the additional inversion for source time and location (Dziewonski et al., 1981) and are routinely provided by the Global CMT Project (http://www.globalcmt.org).

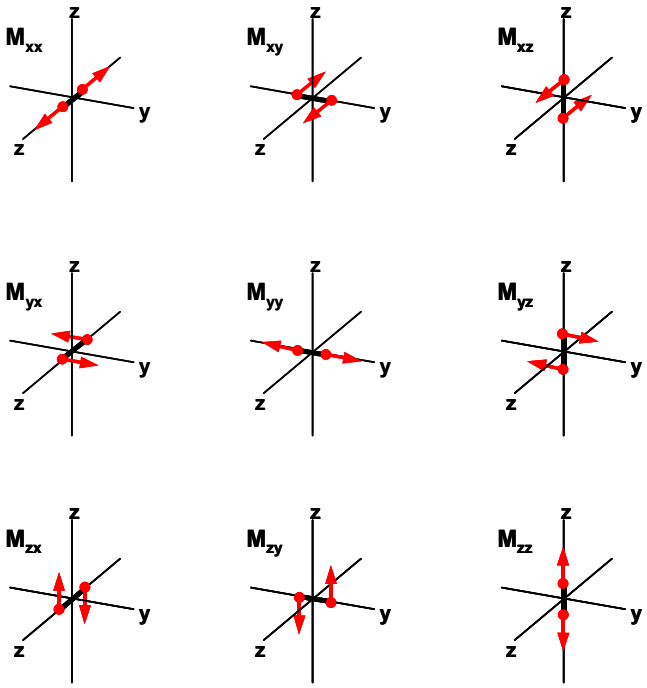

$$\boldsymbol{M} = \begin{pmatrix} m_1 & m_4 & m_5 \\ m_4 & m_2 & m_6 \\ m_5 & m_6 & m_3 \end{pmatrix}.$$

Figure 4: The nine force couples of the seismic moment tensor.

2.1.3. Reliability of fault plane solutions

The quality of either solution, determined by moment tensor inversion or first-motion analysis, depends on the knowledge of the earth structure, since both, the source process and the ray path, determine the waveform data. Thus, an insufficient earth model may lead to mapping unexplainable wave parts into the source, resulting in an erroneous focal mechanism. In general, the quality of the solution depends on the number and the quality of the raw data (polarity readings, signal-to-noise ratio, site-effects) and the geographical distribution of the data points relative to the source. Additionally, methodological limitations are due to different fitting algorithm/error-minimisation procedures and the choice of inversion parameters. Regarding moment tensor inversion, the used frequency-band determines the accuracy of the earth model necessary for a reliable inversion (Barth et al., 2007). While low-frequency recordings (long wavelengths) show effects of large-scale earth structures only, high-frequency waveforms (short wavelengths) are influenced by local hetero-geneities. This all has to be taken into account for estimating the reliability of a fault plane solution.

2.2. Limits of the derivation of stress from FMS

2.2.1. General

The principle axes of the derived moment tensor (P, B, and T) fully describe the focal mechanism and are reported in the WSM database with their azimuth (= dip direction) and plunge (= dip) (in the columns S1AZ, S1PL, S2AZ, S2PL, S3AZ, S3PL). Be aware, that the moment tensor axes of earthquake focal mechanisms are **not** equal to the stress axes! To be strict, the only restriction one can make is that the maximum principal stress (S1) lies within the dilatational quadrant of the focal mechanism (McKenzie, 1969). However, since higher deviations between the P-, B- and T-axes and the principal stress axes S1, S2, and S3 are unlikely they are used as a proxy for the orientation of the stress axes. To account for this inaccuracy, data derived from single focal mechanism (FMS) are given a quality of not better than C regardless of the size of the earthquake and how well the focal mechanism is constraint (see Chapter 6). The limits of stress derivation from FMS are limited by the fault-plane ambiguity and the coefficient of friction:

2.2.2. Fault plane ambiguity

Because of the symmetry of the force double couple and moment tensor on which it is based, the FMS beachball diagram has a crystal-like regularity to it:

- The two nodal planes are perpendicular to each other.
- The pole of the auxiliary plane is colinear with the slip vector on the fault plane.
- The B-axis is coincident with the intersection of the two nodal planes, and so is contained within both of the nodal planes.
- The P-axis is in the middle of the quadrant with dilatational (down) first motions, and the T-axis is in the middle of the quadrant with compressional (up) first motions.
- The T- and P-axes bisect the dihedral angles between the nodal planes; that is, the T- and P-axes are 45° from the nodal planes.
- The P-, T- and B-axes are orthogonal to one another.
- The plane defined by the T- and P-axes also contains the vectors normal to the nodal planes, one of which is the slip vector.

Therefore, on the basis of polarity readings or moment tensor inversion alone, it can not be decided which nodal plane is the fault plane. This can only be decided by calculating higher degree moment tensors (Dahm and Krüger, 1999), the analysis of aftershock distributions (commonly located on the rupture plane), field evidence from surface rupture in case of strong earthquakes, or seismotectonic considerations. Taking into account additional data on azimuthal amplitude and frequency or wave-form patterns, which are controlled by the Doppler effect of the moving source may allow resolving this ambiguity too. The latter can be studied more easily in low-frequency teleseismic recordings while in the local distance range high-frequency waveforms and amplitudes may be strongly influenced by resonance effects due to low-velocity near-surface layers.

2.2.3. Internal friction, stress orientations and possible plate boundary events

One should also be aware that the assumed angle of 45° between the fault plane and S1 and S3 is only true in case of new fracture generation in a homogeneous isotropic medium. In this case the principal axes of the seismic moment tensor (the principal strain axes) would coinside with the principal stress axes. However, this may not be correct in a heterogeneous anisotropic medium (as the crust), a given stress environment and tectonic situation. In by far most cases tectonic earthquakes represent

reactivation of faults in shear. Because of the fault plane ambiguity it is not known a priori which of the two nodal planes of the focal mechanism is the rupture plane and the P-, B- and T-axes are used as a proxy for the orientation of the principal stress axes.

Townend (2006) reviews the difference between P-, B-, T- and S1-, S2-, S3-axes for plate boundary strike-slip faults and shows that these faults are oriented at higher angles to the orientation of maximum horizontal compressive stress S_H than a typical internal friction assumed for the brittle continental crust would suggest. Since earthquakes concentrate on plate boundaries the influence of plate boundary geometry might be dominating the overall kinematics and therefore the inferred "stress" orientations. Plate boundaries are characterized by faults with preferred orientations and presumably include major faults with a low coefficient of internal friction. These faults can not sustain high shear stresses, and thus can be reactivated even when S_H is almost perpendicular to the fault strike (e.g. Zoback et al, 1987). Thus, the orientation of the P-, B-, and T-axis from FMS could deviate considerably from the principal stress orientations. To account for this inaccuracy data derived from FMS are given a quality of not better than C regardless of the size of the earthquake and how well the focal mechanism is constraint. Assuming that major plate boundaries are weak in general, FMS data records in their vicinity are flagged as Possible Plate Boundary Events (PBE) when three criteria are valid:

1. The event is located within a critical distance d_{crit} relative to the closest plate boundary segment. This critical distance depends on the plate boundary type following the global plate boundary type classification of Bird (2003). We estimated d_{crit} by means of a statistical analysis as being 45 km for continental transform faults, 80 km for oceanic transform faults, 70 km for oceanic spreading ridges, and 200 km for subduction zones.
2. The angle between the strike of the nodal plane and the strike of the plate boundary is smaller than 30°.
3. The tectonic regime of the FMS reflects the plate boundary kinematics, i.e. thrust faulting (TF, TS) near subduction zones, strike-slip faulting (SS, NS, TS) near oceanic and continental transforms, and normal faulting (NF, NS) near oceanic spreading ridges.

Stress data records flagged as PBE are not down-ranked in quality and remain as C-quality in the WSM database. By default they are not plotted on stress maps created with CASMO (online database interface; http://www.world-stress-map.org/casmo). For each data record additional information (plate boundary type and distance) is available in the database, which helps the user to evaluate the influence of plate boundary kinematics on the stress orientation at a specific location.

3. Formal stress inversions of focal mechanisms (FMF)

A better estimation of the tectonic stress orientation can be achieved when a set of FMS is available for a region with a homogeneous regional stress field. These mechanisms can be combined to determine the orientations of the principle stress axes by a formal inversion. The formal stress inversion of several FMS improves the quality of stress derivation, but is linked to two main assumptions: (1) It is assumed that the chosen FMS lie in a region with a uniform stress field that is invariant in space and time. The binning technique can be either hypothesis-driven to prove e.g. stress rotations or be data-driven. Hardebeck and Michael (2004) give a detailed discussion on the differences between the binning techniques. To overcome the subjectivity of manual binning Townend and Zoback (2006) used an non-hierarchical clustering algorithm to group FMS in Japan for stress inversion. (2) It is assumed, that the direction of earthquake slip occur in direction of maximum shear stress (Wallace-Bott hypothesis, Bott, 1959).

A stress inversion determines the orientation of the principal stresses that minimises the average difference between the slip vector and the orientation of maximum shear stress on the inverted faults. This angle is commonly called “misfit angle”. Different algorithms of stress inversion have been developed by various authors (the most common routines are described by Gephart and Forsyth, 1984; Michael, 1984; Angelier, 1979; Rivera and Cisternas, 1990). A major difference between stress inversion techniques is the handling of the fault plane ambiguity. Since stress inversion was first used for slickenside field data, some algorithms need the fault plane to be determined a priori. In most cases this is not possible, since further information is to determine the fault plane (see Chapter 2.2.2.). Angelier (2002) provided a method automatically choosing the fault plane. Gephart and Forsyth (1984) perform the inversion as if all nodal planes were independent data, primary and remove the worse fitted auxiliary planes in a second step. The final inversion then includes the planes that are best fitted by a uniform stress field. A third approach applies a bootstrap routine that picks *x* mechanisms at random from the original *x* events. Each dataset than will have some mechanisms repeated two or more times (Michael, 1987). Random decisions of the true fault plane and a variety of bootstrapped datasets finally give a statistical determination of the stress orientation. A recent approach additionally includes a-priori information on the stress field into a probabilistic stress analysis of FMS that accounts for the fault plane ambiguity by calculating probability density functions for the orientations of the principal stress axes (Arnold and Townend, 2007). The different inversion techniques all result in a deviatoric stress tensor, which gives four parameters, the orientation of the three principal stress axes and the relative magnitudes of the intermediate principal stress with respect to the maximum and minimum principal stress. However, stress inversion is not capable of determining stress magnitudes.

The three principal stress axes (reported in the WSM database columns S1AZ, S1PL, S2AZ, S2PL, S3AZ, S3PL) plus the stress ratio of the stress magnitudes RATIO=(S1-S2)/(S2-S3) build up the reduced stress tensor. For the incorporation of new FMF data the specification of RATIO is mandatory. The availability of this information enables to calculate the shape and orientation of the stress ellipsoid and thus the true orientation of S_H. It is recommended to use the formulas given by Lund and Townend (2007) for S_H-determination when the reduced (or full) stress tensor is available.

The adequate binning into regions with a constant stress field in space and time is crucial, but still under debate, especially for regions near to major plate boundaries. Here, dominating fault orientations may distort the inferred stress orientations, what may also count for some intraplate regions. It is still in question, whether plate boundary faults are fundamentally different from smaller intraplate faults. For the discussion of these aspects we refer to the studies of Townend and Zoback (2006) and Hardebeck and Michael (2004).

4. Average or composite focal mechanisms (FMA)

In contrary to a stress inversion, averaging the data or the construction of composite solutions does not take into account the conceptional difference between the stress tensor and the moment tensor (see Chapter 2.2.) and therefore this technique is getting out of use.

4.1. Average focal mechanisms

Despite the fact that the P-axis of a focal mechanism does not necessarily correlate with the orientation of S1, regional compilations show that the average orientation for P-, B-, and T-axes determined from a number of earthquakes gives a good indication of the maximum compressive stress orientation throughout a region (Sbar and Sykes, 1973, Zoback and Zoback, 1980). Because of the circular distribution of P-, B-, and T-axes, they need careful treatment when being averaged, and ignoring the plunge when averaging trends is also problematic (Lund and Townend, 2007).

Anyhow, there are no advantages of an average mechanism compared to FMF since the matter of an adequate binning is relevant for both methods. In future, FMF should be preferred to FMA, since FMF considers the difference between stress tensor and moment tensor, where FMA does not.

4.2. Composite focal mechanisms

When the main shock of an earthquake is only detected within a limited region and the amount and azimuthal distribution of first motions is not sufficient to construct a focal mechanism from this single event, composite focal mechanisms are constructed by superimposing data from aftershocks or other events rupturing the same fault segment (Sbar et al., 1972). For this one major assumption is that all aftershocks used have the same focal mechanism, i.e. have the same radiation pattern, as the main shock. This is reasonable if aftershocks occur along the same fault as the main shock. However, in practice, aftershocks do not necessarily occur along the same fault plane responsible for the main shock. Some aftershocks may occur on faults of a much different orientation from the main shock. Hence, composites rarely show a perfect separation of compressional and dilatational first motions. Aftershocks are often recorded by portable seismic networks from near distance. Superposition requires locating each aftershock in order to calculate ϕ and i_0 for each portable recording station. A composite plot of ray paths cutting the focal sphere is made by moving the centre of the stereonet to the hypocentre of each aftershock. Because of the close recording distance to the aftershock, an upper hemisphere projection of ϕ and i_0 is more convenient. Calculation of the appropriate angle of emergence becomes more critical for larger and deeper earthquakes in areas with a more complex crustal structure.

5. Tectonic stress regime

As the focal mechanism gives information on the faulting type (normal faulting, NF; strike-slip SS; thrust faulting TF), the relative magnitudes of S_H, S_h and S_V are known. Besides the NF, TF, and SS categories, combinations of NF with SS (transtension NS) and TF with SS (transpression TS) exist (Zoback, 1992). NS is appropriate where the maximum stress or P-axis is the steeper plunging of the P- and B-axis. TS is a appropriate where the minimum stress or T-axis is the steeper plunging of the B- and T-axis. The plunges (pl) of P-, B-, and T-axis (or σ_1, σ_2, and σ_3 axis for FMF data records) are used to assign the appropriate stress regime to the data record (see Table 1 and Figure 5).

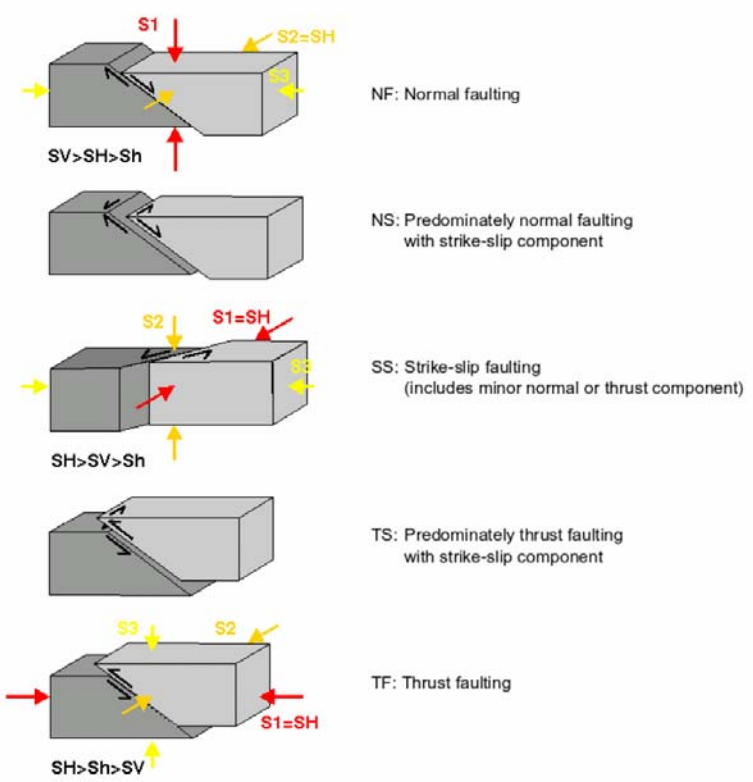

Figure 5: Schematic illustration of the five general tectonic regimes and the according orientations of the principle stress axes (after Anderson, 1951, and Zoback, 1992).

Table 1: Tectonic regime assignment (Zoback, 1992).

P/S1-axis	B/S2-axis	T/S3-axis	Regime	S_H-azimuth
pl > 52		pl < 35	NF	azim. of B-axis
40 < pl < 52		pl < 20	NS	azim. of T-axis + 90°
pl < 40	pl > 45	pl < 20	SS	azim. of T-axis + 90°
pl < 20	pl > 45	pl < 40	SS	azim. of P-axis
pl < 20		40 < pl < 52	TS	azim. of P-axis
pl < 35		pl > 52	TF	azim. of P-axis

The exact cut-off values defining the tectonic regime categories are subjective. Zoback (1992) used the broadest possible categorization consistent with actual P-, B-, and T-axes values. The choice of axes used to infer the S_H orientation is displayed in the table above, e.g. the S_H orientation is taken as the azimuth of the B-axis in case of a pure normal faulting regime (NF) and as 90° + T-axis azimuth in the NS case when the B-axis generally plunges more steeply than the T-axis. The data which fall outside these categories are assigned to an unknown stress regime ("U") and are given an E-quality indicating that the maximum horizontal stress azimuth is not defined.

6. World Stress Map Quality Ranking

All data in the WSM database are quality ranked to facilitate comparison between different indicators of stress orientation (e.g. focal mechanism solutions, drilling-induced tensile fractures, overcoring). The quality ranking criteria for stress orientations determined from focal mechanisms are presented in Tables 2, 3, and 4.

Ideally, the regional stress field would be estimated from a number of events in a given area with a broad azimuthal distribution of fault orientations. The more reliable stress orientation is reflected in the higher WSM quality for the formal inversion of several focal mechanisms (FMF). A-quality data are believed to record the stress orientation to within ±15°, B-quality data to within ±20°. Single focal mechanisms (FMS) are given a C-quality indicating their reliability to within ±25°.

Composite as well as average focal mechanisms (FMA) do not take into account the conceptional difference between the stress tensor and the moment tensor (see chapter 2.2). So they might be even less precise in fault plane orientations than FMS and are assigned to D-quality (reliable within ±40°).

Criteria for down-ranking the WSM quality are:

- a low number of used seismic stations
- large gaps in the azimuthal coverage
- instability of the solution due to minor changes in the dataset or in the inversion parameters
- a high CLVD and/or isotropic part in the moment tensor (Jost and Hermann, 1989)
- a high mathematical standard deviation and data variance

Table 2: World Stress Map quality ranking criteria for formal stress inversions FMF (s.d. = standard deviation).

A-Quality	B-Quality	C-Quality	D-Quality	E-Quality
Formal inversion of ≥ 15 well constrained single event solutions in close geographic proximity and s.d. or misfit angle ≤ 12°	Formal inversion of ≥ 8 well constrained single event solutions in close geographic proximity and s.d. or misfit angle ≤ 20°	-	-	-

Table 3: World Stress Map quality ranking criteria for single focal mechanisms FMS (M = local magnitude).

A-Quality	B-Quality	C-Quality	D-Quality	E-Quality
-	-	• Well constraint single event solution (M ≥ 2.5) • (e.g. CMT solutions)	• Well constrained single event solution (M < 2.5)	• Mechanism with P,B,T axes all plunging 25°-40° • Mechanism with P and T axes both plunging 40°-50°

Table 4: World Stress Map quality ranking criteria for average and composite focal mechanisms FMA.

A-Quality	B-Quality	C-Quality	D-Quality	E-Quality
-	-	-	• Average of P-axis • Composite solutions	• Mechanism with P,B,T axes all plunging 25°-40° • Mechanism with P and T axes both plunging 40°-50°

Acknowledgements

We thank John Townend for helpful discussions that complement and improve these guidelines.

References

Anderson, E.M., 1951. The dynamics of faulting and dyke formation with application to Britain, 2nd ed., Edinburgh, Oliver and Boyd.

Angelier, J., 1979. Determination of the mean principal directions of stresses for a given fault population, Tectonophysics, 56, T17-T26.

Angelier, J., 2002. Inversion of earthquake focal mechanisms to obtain the seismotectonic stress IV - a new method free of choice among the nodal planes, Geophys. J. Int., 150, 588-609.

Arnold, R. and Townend, J., 2007. A Bayesian approach to estimating tectonic stress from seismological data. Geophys. J. Int., 170, 1336-1356.

Barth, A., Wenzel, F. and Giardini, D., 2007. Frequency sensitive moment tensor inversion for light to moderate magnitude earthquakes in eastern Africa. Geophys. Res. Lett., 34, L15302.

Bird, P., 2003. An updated digital model for plate boundaries. Geochem. Geophys. Geosyst., 4(3): 1027, doi:10.1029/2001GC000252.

Bott, M.H.P., 1959. The mechanics of oblique slip faulting. Geol. Mag., 96, 109-117.

Byerlee, J.D., 1978. Friction of rocks. Pure Appl. Geophys., 116: 615-626.

Dahm, T. and Krüger, F., 1999. Higher-degree moment tensor inversion using far-field broad-band recordings: theory and evaluation of the method with application to the 1994 Bolivia deep earthquake. Geophys. J. Int., 137, 35-50.

Dziewonski, A.M., Chou, T.-A. and Woodhouse, J.H., 1981. Determination of earthquake source parameters from waveform data for studies of global and regional seismicity. J. Geophys. Res., 86: 2825-2852.

Gephart, J.W. and Forsyth, D.W., 1984. An Improved Method for Determining the Regional Stress Tensor Using Earthquake Focal Mechanism Data: Application to the San Fernando Earthquake Sequence, J. Geophys. Res., 89, 9305-9320.

Hardebeck, J.L., Michael, A., 2004. Stress orientations at intermediate angels to the San Andreas Fault, California. J. Geophys. Res., 109(B11303): doi:10.1029/2004JB003239.

Jost, M.L. and Hermann, R. B., 1989. A Student's Guide to and Review of Moment Tensors, Seism. Res. Lett., 60, 37-57.

Khattri, K., 1973. Earthquake focal mechanism studies─A review, Earth Sci. Rev., 9, 19-63.

Kisslinger, C., Bowman, J.R., and Koch, K., 1981. Procedures for computing focal mechanisms from local (SV/P) data, Bull. Seism. Soc. Am., 71, 1719–1729.

Lund, B. and Townend, J., 2007. Calculating horizontal stress orientations with full or partial knowledge of the tectonic stress tensor. Geophysical Journal International, 170, 1328-1335.

McKenzie, D.P., 1969. The relation between fault plane solutions for earthquakes and the directions of the principal stress. Bull. Seism. Soc. Am., 59, 591-601.

Michael, A.J., 1984. Determination of stress from slip data: Faults and folds, J. Geophys. Res., 89, 11,517-11,526.

Michael, A.J., 1987. Use of Focal Mechanisms to Determine Stress: A Control Study, J. Geophys. Res., 92, 357-368.

Rivera, L. and Cisternas, A., 1990. Stress tensor and fault plane solutions for a population of earthquakes . Bull. Seism. Soc. Am., 80, 600-614.

Sbar, M.L., Barazangi, M., Dorman, J., Scholz, C.H., Smith, R.B., 1972. Tectonics of the Intermountain Seismic Belt, western United States, Microearthquake seismicity and composite fault plane solutions. Geological Society of America Bulletin, 83: 13-28.

Sbar, M.L., Sykes, L.R., 1973. Contemporary compressive stress and seismicity in eastern North America, An example of intraplate tectonics. Geol. Soc. Am. Bull., 84: 1861-1882.

Stein, S. and Wysession, M., 2003. An introduction to seismology, earthquakes, and earth structure, Blackwell Publishing.

Townend, J. 2006. What do Faults Feel? Observational Constraints on the Stresses Acting on Seismogenic Faults, Earthquakes: Radiated Energy and the Physics of Faulting, Geophysical Monograph Series 170, 313-327.

Townend, J. and Zoback, M.D., 2006. Stress, strain, and mountain building in central Japan. J. Geophys. Res., 111, B03411.

Wallace, R.E., 1951. Geometry of shearing stress and relation to faulting. J. Geol., 59: 118-130.

Zoback, M.L., 1992. First- and second-order patterns of stress in the lithosphere: The World Stress Map project. J. Geophys. Res., 97, 11,703-11,728.

Zoback, M.L., Zoback, M.D., 1980. Faulting patterns in north-central Nevada and strength of the crust. Journal of Geophysical Research, 85: 275-284.

Zoback, M.D., Zoback, M.L., Mount, V.S., Suppe, J., Eaton, J.P., Healy, J.H., Oppenheimer, D.H., Reasenberg, P.A., Jones, L., Raleigh, C.B., I.G., W., Scotti, O., Wentworth, C., 1987. New Evidence of the State of Stress of the San Andreas Fault System. Science, 238: 1105-1111.